Optics Letters

Dissemination of UTC(NIST) over 20 km of commercial optical fiber with active phase stabilization

J. B. VanArsdale,[1] M. J. Deutch,[2] M. A. Lombardi,[2] G. K. Nelson,[2] J. A. Sherman,[2] J. Spicer,[2] W. C. Yates,[2] D. C. Yost,[1] and S. M. Brewer[1,*]

[1]Department of Physics, Colorado State University, Fort Collins, Colorado 80523, USA
[2]National Institute of Standards and Technology, Boulder, Colorado 80305, USA
*samuel.brewer@colostate.edu

Received 7 February 2024; revised 29 March 2024; accepted 3 April 2024; posted 3 April 2024; published 2 May 2024

We demonstrate the transfer of a cesium frequency standard steered to UTC(NIST) over 20 km of dark telecom optical fiber. Our dissemination scheme uses an active stabilization technique with a phase-locked voltage-controlled oscillator. Out-of-loop characterization of the optical fiber link performance is done with dual-fiber and single-fiber transfer schemes. We observe a fractional frequency instability of 1.5×10^{-12} and 2×10^{-15} at averaging intervals of 1 s and 10^5 s, respectively, for the link. Both schemes are sufficient to transfer the cesium clock reference without degrading the signal, with nearly an order of magnitude lower fractional frequency instability than the cesium clocks over all time scales. The simplicity of the two-fiber technique may be useful in future long-distance applications where higher stability requirements are not paramount, as it avoids technical complications involved with the single-fiber scheme.

https://doi.org/10.1364/OL.521175

As frequency standards have seenrapid improvements in stability over the past few decades, the ability to transfer a frequency reference from one location to another without degrading the signal has become of increasing interest in the frequency metrology community. Numerous applications arise from ultrastable frequency transfer, such as precision tests of fundamental physics, the development of long-baseline coherent radio telescope arrays, and proposals for new gravitational wave detectors [1–7]. Optical fiber is one of the most effective media used to distribute stable frequency standards over long distances [6,8]. However, optical fiber is susceptible to thermal and mechanical fluctuations that can significantly limit the performance of the frequency transfer. As Earth undergoes diurnal heating and cooling, an optical fiber link will expand and contract, which yields time variation in the phase delay of a transmitted signal [9]. Further, most commercial telecom optical fibers are placed near highways or railways [10], such that vibrations from vehicular traffic lead to additional phase noise on a transferred signal. A number of techniques have been developed over the past 25 years to compensate for these sources of noise (see Ref. [6] for a review), implementing both active and passive schemes at various levels of complexity and performance [11–28].

To stabilize a fiber link between a local site (with a stable reference) and a remote site, the general procedure is to form a closed optical loop, such that the outgoing and returning phase at the local site can be compared to generate an error signal for a phase-locked loop. In order for the phase-locked loop to ensure the signal at the remote site is exactly equal to the signal at the local site, the system must be symmetric: the phase accumulated on the forward path must be equal to the phase accumulated on the return path [6,16,23]. Unfortunately, this condition is only approximately met for any transfer scheme, as the propagation time of the light enforces an upper limit on the feedback bandwidth. Polarization mode dispersion also imposes feedback limits as light traveling in the forward and reverse directions may not have the same polarization and therefore propagate at different speeds [11]. However, to operate as closely as possible to the symmetry condition, the majority of previously demonstrated fiber links have been implemented on a single optical fiber [1–3,8,11,14,15,18–22,24–26,28,29]. On one fiber, separating the incident and returning light poses complications as backreflections (including Rayleigh, Raman, and stimulated Brillouin scattering) are introduced that can degrade performance [30]. Some schemes avoid this issue by using a slightly different wavelength of light for the return trip and separating the forward and reverse signals with sharp optical bandpass filters (BPFs) [8,14,15,19,20,25,28,29]. However, this technique is still inherently asymmetric, as group velocity dispersion (GVD) causes light at the two wavelengths to travel at different speeds [9]. The forward and backward paths therefore still depend differently on temperature fluctuations, and the fractional frequency instability is largest at an averaging interval of approximately 40,000 s (about half of a day). It has been shown that the fractional frequency instability caused by GVD for a 40 km link with wavelengths separated by 4 nm is on the order of 10^{-17} at an averaging interval of 40,000 s [29]. While this can be an issue for the transfer of optical frequency standards, it is significantly lower than the instability of any microwave frequency standard that has been demonstrated to date and thus

is not a limiting factor in the microwave dissemination schemes considered here.

A simpler scheme, which avoids backreflections altogether, is to use two separate fibers. There is often more than one fiber available in a single bundle, so if we assume that the phase fluctuations are highly correlated in the fibers, then a phase-locked loop will still be sufficient to transfer a frequency reference without significant degradation of stability. In general, this is a good assumption because the two fibers are placed next to each other, so they will experience very similar acoustic noise and temperature fluctuations. In effect, rf transfer over two fibers may not be as stable as a one-fiber technique, but it avoids some complexities in implementation, such as eliminating backreflections and the requirement of an additional laser. Furthermore, the technique is stable enough to transfer signals at the $1 \times 10^{-12}/\sqrt{\tau}$ level, including a secondary UTC(NIST) time scale.

The National Institute of Standards and Technology (NIST) radio station WWV is located in Fort Collins, CO, and contains an ensemble of four cesium beam atomic clocks [31–33]. The output of this ensemble is steered to the primary timescale at NIST and constitutes a secondary representation of UTC(NIST) [34]. In this Letter, we report on the establishment of a dark optical fiber link between NIST radio station WWV and Colorado State University (CSU), with a one-way path of approximately 20 km. We have transferred a radio frequency signal generated by the WWV time scale to CSU by carrier amplitude modulation over this optical fiber link, effectively disseminating the secondary UTC(NIST) representation to CSU. To stabilize this frequency transfer, we use an all-electronic analog feedback technique that consists of readily available and relatively inexpensive components. The technique is tested over the dark optical fiber link, using out-of-loop measurements to characterize the instability of the link itself. We implement both dual-fiber and single-fiber transfer schemes for these out-of-loop measurements and demonstrate that the simpler dual-fiber technique has sufficient stability to transfer the WWV cesium clock signal over all measured time scales (ranging from 1 to 10^5 s).

To compensate for thermal and acoustic noise along the optical fiber path, we implement an all-electronic scheme that utilizes a phase-locked voltage-controlled crystal oscillator (VCXO). One particular benefit of this scheme is that it does not require any physical stretching of the fiber to compensate for changes in the optical path length. The feedback setup is shown in Fig. 1.

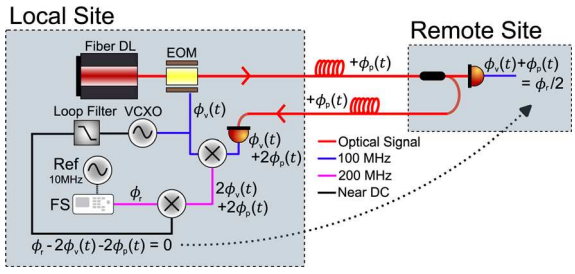

Fig. 1. Electronic scheme implemented for phase-locking a voltage-controlled crystal oscillator (VCXO) to a frequency reference with active compensation of fiber path length fluctuations. The scheme shown here uses two separate fibers and has also been applied to a single-fiber scheme. DL (diode laser), EOM (electro-optic modulator), FS (frequency synthesizer).

At the local site, a diode laser is amplitude-modulated with an electro-optic modulator driven by a 100 MHz VCXO, which has a tunable phase $\phi_v(t)$. This light is sent over the dark telecom optical fiber to the remote site. The fiber is primarily underground, with approximately 18 km buried and 2 km aerial. Along this fiber, a phase $\phi_{p_1}(t)$ is accumulated, which is a function of time due to temperature fluctuations and vibrational noise on the fiber. Some of this modulated light is sampled to generate the transferred reference, and the rest is sent back to the local site. The signal accumulates an additional phase $\phi_{p_2}(t)$ on the trip back, which we assume to be approximately equal to $\phi_{p_1}(t)$ because the fibers are contained within the same bundle. We then mix the returning signal with the modulation signal (from the VCXO, with phase $\phi_v(t)$) and apply a bandpass filter to isolate a signal at 200 MHz with phase $2\phi_v(t) + 2\phi_{p_1}(t)$. A frequency synthesizer referenced to a frequency standard at the local site is used to generate a 200 MHz signal with phase ϕ_r, which has the same fractional frequency instability as the frequency standard. This signal is used for homodyne phase detection of the 200 MHz bandpassed signal (i.e., a double-balanced mixer and low-pass filter (LPF)). The error signal is further conditioned with a proportional–integral (PI) servo and sent to the VCXO to form a phase-locked loop. In the locking condition, time dependence of the error signal is driven to zero, such that

$$\phi_r - 2\phi_v(t) - 2\phi_{p_1}(t) = 0. \quad \textbf{(1)}$$

When locked, the remote site has a signal with *constant* phase,

$$\phi_v(t) + \phi_{p1}(t) = \phi_r/2. \quad \textbf{(2)}$$

Hence, we effectively transfer the reference signal with phase compensation. We use this technique to disseminate the secondary UTC(NIST) time scale from radio station WWV (local site) to CSU (remote site). We refer to this UTC(NIST) time scale at WWV as CRFS (cesium-referenced frequency standard). We characterized the performance of the fiber transfer with a heterodyne measurement against a commercial rubidium frequency standard. This frequency standard consists of a 10 MHz crystal oscillator locked to the 6.8 GHz hyperfine transition in rubidium and is additionally steered by a 1 pulse-per-second (1 PPS) Global Positioning System (GPS) signal. We will refer to this standard as RRFS (rubidium-referenced frequency standard). The schematic for the CRFS–RRFS comparison is shown in Fig. 2. The transferred CRFS signal at 100 MHz is bandpass filtered and divided down to 10 MHz. This signal is used as the

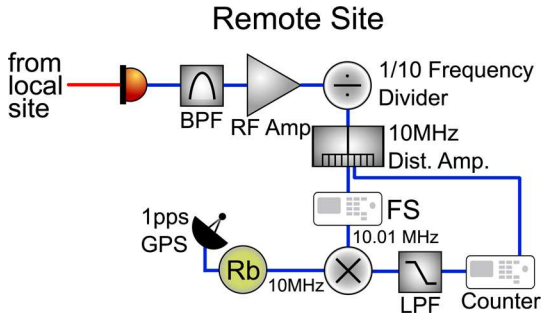

Fig. 2. Electronic scheme at the remote site (CSU) for measurements comparing a GPS-disciplined rubidium clock to the transferred cesium frequency standard. A frequency synthesizer (FS) and frequency counter are both referenced to the cesium standard. BPF (bandpass filter), RF amp (radio frequency amplifier), dist. amp (distribution amplifier), LPF (low-pass filter).

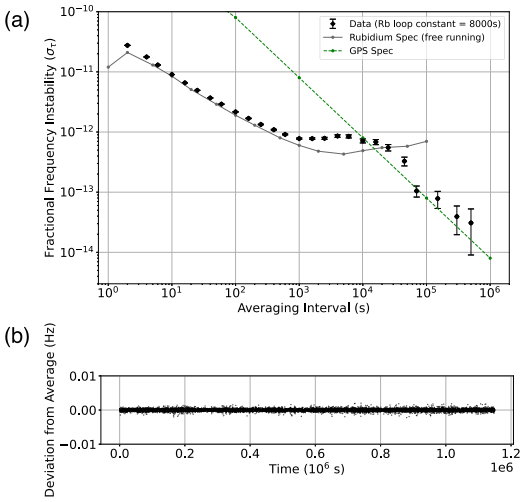

Fig. 3. (a) Allan deviations of our commercial rubidium clock vs. the NIST WWV cesium time scale. (b) Long-term CRFS-RRFS comparison data taken for a RRFS steering time constant of 8000 s. Deviations are relative to the 10 kHz sampled beat note. The link remains locked over the entire measurement period of approximately two weeks.

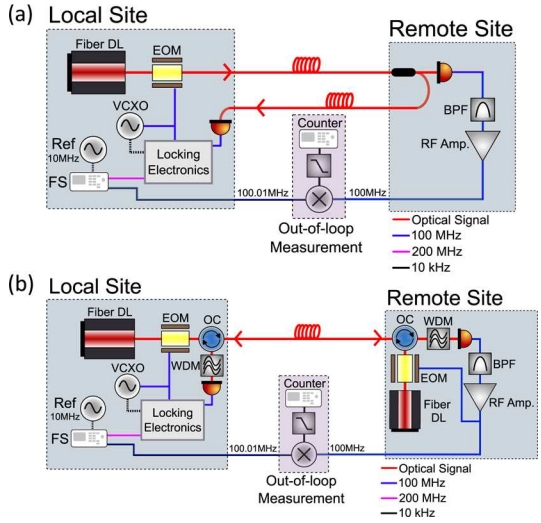

Fig. 4. (a) Dual-fiber scheme and (b) single-fiber scheme for out-of-loop measurements of the link performance. In these measurements, the local and remote sites are at the same physical location and set up in a loop-back arrangement where each length of fiber has been effectively doubled. The locking electronics consist of components detailed in Fig. 1. The FS and frequency counter are both referenced to the RRFS. DL (diode laser), EOM (electro-optic modulator), OFS (optical fiber splitter), PD (photodiode), BPF (bandpass filter), RF amp (radio frequency amplifier), LPF (low-pass filter), DBM (doubly balanced mixer), VCXO (voltage-controlled oven-controlled crystal oscillator), OC (optical circulator), WDM (wavelength division multiplexer), FS (frequency synthesizer).

input to a distribution amplifier and sent as a reference to both a frequency synthesizer and a frequency counter. The frequency synthesizer generates a signal at 10.01 MHz, which is down-converted to 10 kHz upon mixing with the 10 MHz output of the RRFS. We then input this 10 kHz signal to the frequency counter for data logging at a 1 s gate time.

Allan deviations of these measurements are shown in Fig. 3(a), along with specifications of the RRFS and 1 PPS GPS instabilities. Figure 3(b) shows a long-term measurement of the 10 kHz beat note for a period over 10^6 s (about 2 weeks). This demonstrates the robustness of the technique: in fact, the link has remained locked for over 6 months to continuously transfer the CRFS signal from WWV to CSU. To characterize the extent of additional phase noise incurred on the dual-fiber scheme relative to the single-fiber scheme, we performed out-of-loop measurements of both techniques. These measurements were configured in a loop-back arrangement, such that both the local and remote measurement sites are at the same physical location. The total optical path from the local to the remote site is one round trip from CSU–WWV–CSU, which is approximately 40 km, effectively doubling the length of each fiber that was used in the transfer of the CRFS signal. This configuration allows us to directly compare the phase at the remote site with the phase at the local site to measure the instability of the (actively stabilized) link itself. Schematics for these two schemes are shown in Fig. 4. In the dual-fiber scheme, we sample 10% of the light received at the remote site (after traveling from CSU–WWV–CSU), amplify it through an erbium-doped fiber amplifier, and send the light back to the local site through separate fibers in the same bundle (again traveling from CSU–WWV–CSU) [33]. In the single-fiber scheme, we detect all of the modulated light received at the remote site and use this signal to modulate a second laser at a different optical frequency, which is sent back to the local site on the same fiber using optical circulators.

A dual-output phase-locked frequency synthesizer referenced to our RRFS generates the 200 MHz reference signal. The second output of this frequency synthesizer is set to 100.01 MHz and mixed with the locked 100 MHz signal to generate a 10 kHz signal for high-resolution heterodyne counting on a frequency counter (also referenced to the RRFS). The input power to the telecom optical fibers is kept to approximately 5 mW, below the threshold for Brillouin scattering [30]. For the dual-fiber scheme, we use a 1554.13 nm fiber-coupled diode laser, along with a birefringent fiber loop for polarization control. For the single-fiber scheme, we additionally use a 1550.12 nm single frequency fiber laser at the remote site and employ wavelength division multiplexers before the local and remote photodiodes to filter out back reflections [33]. Allan deviations of these schemes are shown in Fig. 5, along with the noise floor of the technique, measured by using a short 5 m optical fiber in place of the fiber link. Also plotted is the instability of a free-running link over 40 km of the optical fiber and the cesium beam clock instability specification. We observe a fractional frequency instability of $1.1 \times 10^{-12}/\sqrt{\tau}$ and $1.5 \times 10^{-12}/\sqrt{\tau}$ for the single-fiber and dual-fiber schemes, respectively, compared to $6.0 \times 10^{-12}/\sqrt{\tau}$ for the unstabilized link. The instability of the single-fiber scheme is likely limited by the 2 km portion of aerial fiber in the link. Performing the transfer at a higher modulation frequency would help suppress the noise floor. The dual-fiber scheme performs worse than the single-fiber scheme for averaging intervals larger than approximately 10 s, before converging again near an averaging interval of 1 day (84,000 s). Thermal effects are most pronounced in the dual-fiber scheme on time scales on the order of 1 h. Even with additional thermal noise, the instability introduced by the dual-fiber scheme remains significantly lower than the instability of the cesium beam clock ensemble and is sufficient to transfer the CRFS. We note that since these out-of-loop measurements use

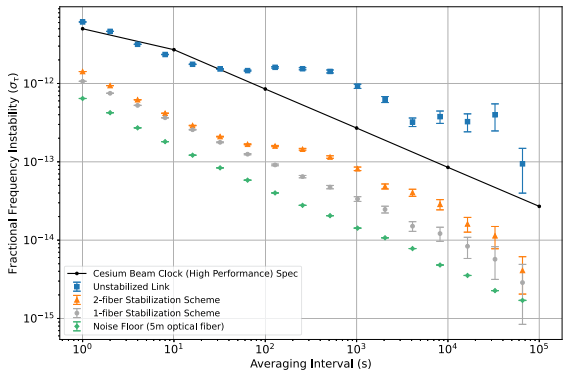

Fig. 5. Allan deviations for out-of-loop measurements. Frequency data centered at 10 kHz is used for all of these plots. Each set of data was measured over approximately 200,000 s at the same time of the week (Friday–Monday) to ensure similar vehicular traffic conditions. One set of data was taken at a time, such that the measurement campaign lasted a total of 4 weeks. Also shown is the specification for the cesium beam clock with a high-performance beam tube.

a fiber link which is effectively twice as long as the link used for transfer of the CRFS signal from radio station WWV, the fractional frequency instabilities for the shorter link are a factor of 2 lower in our actual transfer. However, WWV has an averaged ensemble of four cesium beam clocks, so the instability of these clocks is likely a factor of $\sqrt{4} = 2$ lower than shown on the specification in Fig. 5. Thus, even with these considerations, a dual-fiber scheme has the ability to transfer frequency references at the $1 \times 10^{-12}/\sqrt{\tau}$ level.

In conclusion, we have demonstrated the distribution of a secondary UTC(NIST) time scale over commercial telecom optical fiber, utilizing a simple all-electronic active stabilization scheme. Out-of-loop measurements indicate that a single-fiber scheme is more effective at eliminating instability from slow temperature fluctuations than a dual-fiber scheme, but either is sufficient to transfer the radio station WWV time scale signals. Further, the dual-fiber scheme is more robust against unlocking, as very little equipment is required at the remote site. This dual-fiber scheme also avoids complications and costs involved in a single-fiber scheme, including a second laser, a modulator, and the challenge of mitigating backreflections. We note that a dual-fiber scheme may not always be possible since dark fibers tend to be a scarce resource, but often fibers are laid in bundles, where more than one is available. Out-of-loop measurements on a 40 km one-way link demonstrate that radio frequency standards with frequency instabilities on the order of $1 \times 10^{-12}/\sqrt{\tau}$ can be transferred over similar distances with a dual-fiber technique while maintaining phase coherence, without appreciable degradation of stability. Future work can investigate the effects of polarization mode dispersion on the fiber transfer, including the implementation of a polarization scrambler to possibly improve the frequency instability. This work indicates the feasibility for the development of a US-based optical fiber network for frequency metrology and possible quantum networking applications using existing fiber infrastructure.

Funding. National Institute of Standards and Technology (70NANB 22H218); Office of Naval Research (N00014-22-1-2070); National Science Foundation (PHY-2110102, PHY-2207298); Colorado State University.

Acknowledgment. We thank C. Sanner, Y.-S. Li-Baboud, D. H. Slichter, and A. Novick for their careful reading of the manuscript.

Disclosures. The authors declare no conflicts of interest.

Data availability. Data underlying the results presented in this paper are not publicly available at this time but may be obtained from the authors upon reasonable request.

REFERENCES AND NOTE

1. A. Matveev, C. G. Parthey, K. Predehl, *et al.*, Phys. Rev. Lett. **110**, 230801 (2013).
2. J.-F. Cliche and B. Shillue, IEEE Control Syst. **26**, 19 (2006).
3. M. Calhoun, R. Sydnor, and W. Diener, "A stabilized 100-megahertz and 1-gigahertz reference frequency distribution for Cassini radio science," IPN Progress Report 42 (Jet Propulsion Laboratory, Pasadena, California 2002).
4. F. Riehle, Nat. Photonics **11**, 25 (2017).
5. M. Calhoun, S. Huang, and R. L. Tjoelker, Proc. IEEE **95**, 1931 (2007).
6. S. M. Foreman, K. W. Holman, D. D. Hudson, *et al.*, Rev. Sci. Instrum. **78**, 021101 (2007).
7. K. Beloy, M. I. Bodine, T. Bothwell, *et al.*, Nature **591**, 564 (2021).
8. P. Krehlik, L. Sliwczynski, L. Buczek, *et al.*, IEEE Trans. Ultrason., Ferroelect., Freq. Contr. **63**, 993 (2016).
9. A. Walter and G. Schaefer, in *Optical Fiber Communication Conference* (Optical Society of America, 2002), paper WU4.
10. R. Durairajan, P. Barford, J. Sommers, *et al.*, *Proceedings of the 2015 ACM Conference on Special Interest Group on Data Communication* (2015), pp. 565–578.
11. O. Lopez, A. Amy-Klein, M. Lours, *et al.*, Appl. Phys. B **98**, 723 (2010).
12. G. Marra, H. S. Margolis, S. N. Lea, *et al.*, Opt. Lett. **35**, 1025 (2010).
13. K. W. Holman, D. D. Hudson, J. Ye, *et al.*, Opt. Lett. **30**, 1225 (2005).
14. F. Narbonneau, M. Lours, S. Bize, *et al.*, Rev. Sci. Instrum. **77**, 064701 (2006).
15. Q. Li, L. Hu, J. Zhang, *et al.*, IEEE Photonics Technol. Lett. **33**, 660 (2021).
16. L-S. Ma, P. Jungner, J. Ye, *et al.*, Opt. Lett. **19**, 1777 (1994).
17. J. Ye, J.-L. Peng, R. J. Jones, *et al.*, J. Opt. Soc. Am. B **20**, 1459 (2003).
18. M. T. L. Hsu, Y. He, D. A. Shaddock, *et al.*, IEEE Photonics Technol. Lett. **24**, 1015 (2012).
19. C. Liu, J. Shang, Z. Zhao, *et al.*, IEEE Photonics J. **13**, 7100108 (2021).
20. S. Wang, D. Sun, Y. Dong, *et al.*, Opt. Lett. **39**, 888 (2014).
21. X. Wang, Z. Liu, S. Wang, *et al.*, Opt. Lett. **40**, 2618 (2015).
22. L. Zhang, L. Chang, Y. Dong, *et al.*, Opt. Lett. **36**, 873 (2011).
23. L. Primas, G. Lutes, and R. Sydnor, in *Proceedings of the 42nd Annual Frequency Control Symposium*, 1988, (IEEE, 1988), pp. 478–484.
24. S. Schediwy, D. Gozzard, S. Stobie, *et al.*, Opt. Lett. **42**, 1648 (2017).
25. Ł. Sliwczynski, P. Krehlik, Ł. Buczek, *et al.*, IEEE Trans. Instrum. Meas. **60**, 1480 (2011).
26. B. Ning, P. Du, D. Hou, *et al.*, Opt. Express **20**, 28447 (2012).
27. C. Daussy, O. Lopez, A. Amy-Klein, *et al.*, Phys. Rev. Lett. **94**, 203904 (2005).
28. M. Kumagai, M. Fujieda, S. Nagano, *et al.*, Opt. Lett. **34**, 2949 (2009).
29. L. Yu, R. Wang, L. Lu, *et al.*, Opt. Express **23**, 19783 (2015).
30. M. Damzen, V. Vlad, A. Mocofanescu, *et al.*, *Stimulated Brillouin Scattering: Fundamentals and Applications* (CRC Press, 2003).
31. M. Lombardi, "NIST time and frequency services," NIST Special Publication 432.
32. J. Levine, Metrologia **45**, S23 (2008).
33. Identification of a product herein is for documentation purposes only, and does not imply recommendation or endorsement by NIST, nor does it imply that this product is necessarily the best available for the purpose.
34. J. Levine, in *Proceedings of the 40th Annual Precise Time and Time Interval Systems and Applications Meeting* (2008), pp. 205–218.